EQUATIONS OF STATE AND THERMOPHYSICAL PROPERTIES OF SOLIDS UNDER PRESSURE

WILFRIED B. HOLZAPFEL
Physics Department
University Paderborn
33095 Paderborn / Germany

1. Introduction

Equations of State (EOS) for a given thermodynamic system are usually considered to represent relations between the pressure, p, the volume, V, and the temperature, T, in the form p = p(V,T) or V = V(p,T). In most cases only the isothermal relations $p = p_T(V)$ or $V = V_T(p)$ are studied experimentally. Therefore in most cases only "parametric" EOS forms are discussed, in which the experimentally determined parameters for the volume $V_0(T)$, for the bulk modulus $K_0(T)$ and for its first and higher order pressure derivatives $K_0'(T)$, $K_0''(T)$, …., represent the values for ambient (zero) pressure at the given temperature T. Different isotherms are thereby represented usually by the same parametric EOS form with only different values for $V_0(T)$, $K_0(T)$, $K_0'(T)$,….

A question often asked is, which analytic form should be used for a parametric EOS, and what are the differences between different common analytic forms? These and similar questions will be discussed together with a review of the most common parametric EOS forms for solids in section 2.

More generally, however, the rigorous definition of an EOS starts from thermodynamic potentials (Gibbs functions) like the (Helmholtz) free energy, F(V,T,N,…) or the (Gibbs) free enthalpy, G(p,T,N,…), or the internal energy, U(V,S,N…), or the enthalpy H(p,S,N,…), in which N represents the total particle number, S stands for the entropy and the dots leave space for other thermodynamic variables like uniaxial stress or strain, electric and magnetic field strength and electric or magnetic polarisations. One should note that the functions F, G, U, and H are "thermodynamic potentials" giving complete characterisations of the "system" only with respect to "canonical" variables as given in their definitions above. All the partial derivatives also known as Maxwell relations define pairs of canonical variables:

$$p(V,T) = -\,\partial F(V,T)/\partial V\big|_T \qquad S(V,T) = -\,\partial F(V,T)/\partial T\big|_V$$
$$V(P,T) = \partial G(p,T)/\partial p\big|_T \qquad S(p,T) = -\,\partial G(p,T)/\partial T\big|_p$$
$$p(V,S) = -\,\partial U(V,S)/\partial V\big|_S \qquad T(V,S) = \partial U(V,S)/\partial S\big|_V$$
$$V(p,S) = \partial H(p,S)/\partial p\big|_S \qquad T(p,S) = \partial H(p,S)/\partial S\big|_p$$

Just for clarity, the thermodynamic variables have been restricted here to the canonical pairs p-V and S-T.

Like p = p(V,T) all the other Maxwell relations can be considered as "equations of state" in a more general sense: the system, or in other words the material, determines the special form of the EOS, not only for p = p(V,T) but also for any of the other relations, and each of these Maxwell relations gives only a partial description of the

thermodynamic system. To recover from the p(V,T)-EOS the thermodynamic potential F(V,T) requires additional knowledge about the (caloric) S(V,T)-EOS and in addition one reference point for F(V,T) to fix one remaining constant of integration.

These general relations between "equations of state" and thermodynamic potentials are elaborated more or less clearly in any of the standard textbooks on statistical mechanics and thermodynamic. My favoured author for this subject is G. Falk [1].

The link from the p(V,T)-EOS to a quantum mechanical description of the many body system is provided by the partition function Z(V,T) = exp(-F(V,T)/(kT)) and the use of this link will help us in section 3 to go beyond a parametric p(V,T)-EOS formulation. This approach is usually related to the "Mie-Grüneisen" approximation. The advantages as well as the limitations of this MG-approximation are worked out in section 3, which forms the basis for a software package to fit in a self consistent way not only several isotherms on the basis of ambient pressure data for $V_0(T)$ and $K_0(T)$ but also by including specific heat data $C_{p0}(T)$ (and if available also thermal expansivity data $\alpha_0(T)$). In this way the physical background for the dependence of the "thermal pressure" on volume and temperature is explored and the volume dependence of parameters like the Debye temperature $\theta(V)$ and some extra anharmonicity parameter A(V) are determined to be used in a second software package for the forward calculation of not only different p(V,T) isotherms but also all the other thermo-physical properties mentioned so far. The details of these software packages are presented in section 4. Section 5 is devoted to a critical discussion of the advantages and limitations of the present approach.

2. Parametric EOS forms

2.0 GENERAL REMARKS

Many different parametric EOS forms have been listed and discussed in the literature [2-10]. Therefore only a few specific aspects of the most common forms are discussed here with special attention to the question as to whether there is any special advantage in one of these forms with respect to the others.

For instance it can be a special advantage for some applications if the form can be inverted analytically from p(V) to V(p). However, none of the "invertible EOS" forms given in the literature [10-14] and discussed in the next section 2.1 gives a finite value for the cohesive energy upon integration, and this is considered as a serious deficiency.

On the other hand EOS relations derived from finite strain theory, discussed in section 2.2, result in finite values for the cohesive energy only if the definition of the strain $\varepsilon = (1-(V/V_0)^{n/3})/n$ has $n < 0$ keeping the generalized strain finite at infinite expansion ($V/V_0 \rightarrow \infty$). With $n = -2$ one obtains the well-known Birch-Murnaghan equation [15], which is compared with other forms from finite strain theory in section 2.2.

A third approach, discussed in section 2.3, starts from "effective" two-body potentials, well known from atomic and molecular physics. These forms always imply a finite value for the cohesive energy, but mostly do not provide a series expansion with as many free parameters as needed for accurate representations of the experimental data. Without the modification by a series expansion, none of these forms deserves the label "universal" and, as shown in the comparison of the different parametric forms in section

2.4, the "universal EOS" promoted by Vinet et al. [16] is not only limited by its few free parameters but also by the fact that it is "universally" wrong at strong compression, because it diverges with respect to the well known limiting behaviour for all kinds of solids at very strong compression [7,8,10,17-20]. This observation leads to new, more reasonable, forms presented in section 2.4.

2.1 INVERTIBLE EOS FORMS

Murnaghan [11,12] derived the most commonly used invertible EOS form:

$$p = (K_0 / K_0') \cdot ((V_0 / V)^{K_0'} - 1) \quad \text{or} \quad V = V_0 \cdot (1 + (K_0' / K_0) \cdot p)^{-1/K_0'} \tag{1}$$

This form is called here MU2 and can be obtained by integration from the bulk modulus

$$K(p) = K_0 + K_0' \cdot p \tag{2}$$

with the assumption that K_0' is constant or K(p) is a linear function of pressure. This assumption is reasonable for moderate compressions of a few percent, but leads rapidly at strong compression to large discrepancies either in the fitted values for K_0 and K_0' with respect to the correct zero pressure values, or in extrapolations on the basis of the correct zero pressure values for K_0 and K_0' with respect to the experimental p-V-data.

A slight improvement is obtained if one allows for a finite value of the next higher order pressure derivative K_0'' in this series expansion, which results [13] in the invertible (third order) Freund-Ingalls form FI3:

$$p = 1/b \cdot \left[\exp((1/a) \cdot (1 - (V/V_0)^{1/c}) - 1\right] \quad \text{or} \quad V = V_0 \cdot \left[1 - a \cdot \ln(1 + b \cdot p)\right]^c \tag{3}$$

with $a = (1 + K_0')/(1 + K_0' + K_0 K_0'')$, $b = (K_0' / K_0) - K_0''/(1 + K_0')$ and $c = (1 + K_0' + K_0 K_0'')/(K_0'^2 + K_0' - K_0 K_0'')$ another third order invertible EOS form has been derived by a different assumption about the pressure dependence of the bulk modulus [14] with the additional parameter β:

$$K(p) = K_0 (1 + p \cdot K_0' / (\beta \cdot K_0))^{\beta} \tag{4}$$

Upon integration one obtains the form BC3:

$$p = K_0 \cdot (\beta / K_0') \cdot \left[(1 - (1-\beta) \cdot (K_0' / \beta) \cdot \ln(V/V_0))^{1/(1-\beta)} - 1\right] \quad \text{or}$$

$$V = V_0 \cdot \exp\left[\beta / ((1-\beta) \cdot K_0') \cdot (1 - (1 + p \cdot K_0' / (\beta \cdot K_0))^{1-\beta})\right] \tag{5}$$

in which $p_{sp} = -K_0 \cdot (\beta / K_0')$ and $V_{sp} = V_0 \cdot \exp[\beta / ((1-\beta) \cdot K_0')]$ have been described as pseudo-spinodal pressure and volume that characterise an instability at $p_{sp} < 0$.

None of the forms MU2, FI3 or BC3 gives a finite value for the cohesive energy upon integration to $V \to \infty$ and the limiting behaviour at strong compression is not improved by FI3 or BC3 with respect to MU2. Therefore these forms are only useful for very moderate compressions (or expansions) and lead rapidly to serious errors in any extrapolation of these forms beyond the range of moderate compression.

2.2 FINITE STRAIN EOS RELATIONS

If one uses a macroscopic theory of finite strain for the elastic deformation energy of a solid body, the corresponding "finite strain EOS" depends not only on the order of the

series expansion for the total elastic energy, but also on the definition of the strain, which is given in generalised form by

$$\varepsilon = (1-(V/V_0)^{n/3})/n \tag{6}$$

Thereby V_0 is the volume of the reference state, V is the volume under pressure, n = 2 represents Lagrangian strain, and n = -2 Eulerian strain. Birch [15] preferred the Eularian strain for various reasons and the Lth order form BEL:

$$p_{BEL} = (3/2)\cdot K_0 \cdot x^{-7}\cdot(1-x^2)\cdot(1+\sum_2^L c_k \cdot (x^{-2}-1)^{k-1}) \tag{7}$$

(The "order" L in my nomenclature [7,8,10] is reduced by 1 with respect to the order of the strain energy form to count the free parameters as in the other forms of section 2.) The case of n = 0 on the other hand can be represented by the logarithmic or Hencky strain [9]:

$$\varepsilon = -(1/3)\cdot \ln(V/V_0) \tag{8}$$

which avoids the divergence to negative values of p at strong compression typical for the second order Birch form BE2 with $K_0' < 4$. However no series expansion with this logarithmic strain gives finite values for the cohesive energy and neither the correct asymptotic behaviour at $V \to 0$. This fact has been noticed already by Stacey [21], where the only EOSs with the correct asymptotic value $K_\infty' = 5/3$ were my forms [7,8, 10] to be discussed under the labels HOL, H1L and APL below.

If one supposes that any "reasonable" EOS form should give a finite value of the cohesive energy, one must restrict the values of n in the strain relation to n < 0. The special choice of n = -2 selected by Birch [15] was obviously motivated by two observations:

I. The first order form BE1 for the (quadratic) Eulerian strain results in a value of $K_0' = 4$, which represent a good average value for the materials considered by Birch.

II. In fact, BE1 corresponds to an effective interatomic potential for dense packed monatomic solids with power laws for the repulsive and attractive potential parts with the powers 4 and 2 respectively. These values give a good compromise between a larger value for the repulsive term, a smaller value for the attractive term, and the requirement to avoid an unphysical turnover to negative pressures at strong compression.

The higher order Birch forms BEL may be considered as just resulting from modified effective power law potentials, which are discussed in detail in the next section, where it is also shown that BEL represents a good compromise between reasonable physical requirements and a simple functional form.

2.3 EFFECTIVE POTENTIAL EOS FORMS

Mie [22] introduced already in 1903 the idea that the balance between attractive and repulsive atomic forces determines the elastic properties of solids at ambient conditions. He proposed to use two power laws with just a steeper exponent for the repulsive force. This form for the interatomic potential can be summed over all lattice sites for dense packed monatomic solids without the need for any new parameters and results with three free parameters K_0, m and n in a third order EOS labelled here Mi3:

$$p = (3/n)\cdot K_0 \cdot (V/V_0)^{-m/3}\cdot(1-(V/V_0)^{n/3}) \tag{9}$$

This form gives $K_0' = (2m-n)/3$ and for the cohesive energy

$$E_0 = \frac{9 \cdot V_0 \cdot K_0}{(m-3)(m-3-n)} = \frac{9 \cdot V_0 \cdot K_0}{(m-3)(3K_0' - m - 3)} \tag{10}$$

These relations allow both E_0 and K_0' to be determined independently. This form corresponds also to BE1 for m = 7 with n = 2. One should note in addition that the Mie potential was later often referred to as the Lennard-Jones [23] potential.

Also at the beginning of the last century it was realised that the repulsive term of interatomic potentials is probably better modelled by an exponential term either in combination with a power law (Born-Mayer potential, [24]) or with a second exponential (Morse potential [25]) or a combination of one exponential with a power law series (Rydberg potential [26]). The use of an effective Rydberg-potential with only nearest neighbour interactions for a dense packed monatomic solid results in the effective Rydberg form (of second order) ER2, which is given most conveniently with $x = (V/V_0)^{1/3}$ and $c_{ER2} = (2/3)(K_0' - 1)$ by

$$p_{ER2} = 3 \cdot K_0 \cdot (1-x) \cdot x^2 \cdot \exp(c_{ER2} \cdot (1-x)) \tag{11}$$

This form was published first by Stacey et al [3] and was later advertised as a "universal EOS" by Vinet et al [16] without reference to either Rydberg or Stacey et al.. It was never admitted that this form represents just a reasonable approximation for a limited range in compression. The different behaviour of solids under strong compression, well known from many theoretical studies [17-20] was ignored by Vinet et al. Therefore the only "universal" property of ER2 is obviously the fact, that it is "universally wrong" at strong compression and "universally right" only in the trivial sense of a reasonable approximation for moderate compression like Hooke's law for infinitesimal strain. In any case, serious scientists would use the word "universal" somewhat more carefully in any context. Finally Vinet et al. had anyhow to admit [27] that the ER2 form needs modifications for strong compressions and a series expansion in terms of $(1-x)^n$ in the exponent of ER2 was introduced as improvement, but this modification did not remove the critical divergence. On the contrary, the integrability of ER2 with its simple form for the cohesive energy

$$E_0 = 9 \cdot V_0 \cdot K_0 / c_{ER2}^2 = 4 \cdot V_0 \cdot K_0 / (K_0' - 1)^2 \tag{12}$$

was lost.

Stimulated by the nonsense of a "universal EOS forms" I started with a modification of the ER2 form, using the correct exponent -5 for the leading x^{-2} term in eq. 11. With this exponent -5 the divergence with respect to the Fermi gas behaviour at very strong compression was removed [28], but this form labelled H0L did not yet constrain the prefactor to the value of the Fermi gas. Therefore, one additional constraint was introduced in the later form H1L, constraining the parameter c in the exponent to the value $c_0 = -\ln(3 \cdot K_0 / p_{FG0})$. The parameter $p_{FG0} = a_{FG} \cdot (Z/V_0)^{5/3}$ represents the pressure of a Fermi gas with the total electron number Z in the (atomic) volume V_0 and $a_{FG} = 0.02337 \text{GPa} \cdot \text{nm}^5$ is a universal constant for the Fermi gas.

Due to the fact that the form H1L retained some similarity to the modified Vinet form, it could not be integrated in closed form. It has therefore been replaced [8] by the form APL, an **A**dapted **P**olynomial expansion of the order **L**, given by

$$p_{APL} = 3 \cdot K_0 \cdot x^{-5} \cdot (1-x) \cdot \exp(c_0 \cdot (1-x)) \cdot \left(1 + x \cdot \sum_2^L c_k \cdot (1-x)^{k-1}\right) \tag{13}$$

where $c_0 = -\ln(3 \cdot K_0 / p_{FG0})$ constrains the form at very strong compression to the (theoretical) Fermi gas behaviour. This series expansion allows for closed form integration and good convergence in fitting of experimental data. The parameters c_2, c_3, …..c_L can be related to the different pressure derivatives of the bulk modulus at ambient conditions, K_0', K_0'', …, and to the cohesive energy E_0. For the first order form AP1 one finds for instance [29]:

$$K_0' = 3 + (2/3) \cdot c_0 \quad \text{and} \quad E_0 = (9/2) \cdot V_0 \cdot K_0 \cdot \left((2 + c_0)(1 - c_0 \cdot e^{c_0} \cdot E1(c_0)) - 1 \right) \qquad (14)$$

with the well-known exponential integral function $E1(x) = \int_x^\infty e^{-t} / t \cdot dt$.

The values for c_0 vary from 1 for the light metals to 4 for the heavier metals with 7 for Cs. Values around 5 are also found for all the rare gas solids [30]. Since the first order relation (eq. 14) gives a strong correlation of K_0' with c_0 one can expect typical values of K_0' for the lighter metals in the range of 4, for the heavier metals in the range of 5 to 6 and for the rare gas solids in the range of 6 to 7, which corresponds to a very reasonable first order correlation in contrast to the purely empirical assumption of $K_0' = 4$ for the first order form BE1. Further details of this correlation and the explicit calculation of the cohesive energy up to the fourth order form AP4 are given in the corresponding literature [31].

Finally, one may recall that the higher order Birch equation BEL can also be related to a microscopic interatomic potential for densely packed monatomic solids. In this case the interatomic potential is given by a power series in $x^{-2k-3} = (V/V_0)^{-(2/3) \cdot k - 1}$ starting with the attractive term x^{-3} and ending with the highest power x^{-2L-5}, which is repulsive only if the value for the corresponding c_{BEL} in p_{BEL} (eq. 8) is positive. c_{BE2} for the second order form BE2 is positive only for $K_0' > 4$. Therefore, $K_0' < 4$ corresponds in this case to the strange situation that the term with the highest (negative) power is an attractive term. This limitation of the Birch form BEL is discussed further below in a comparison of the different forms by the use of a special "linearisation scheme".

2.4 COMPARISON OF LINEARISED FORMS

In the last section it was noted that most of the common parametric EOS forms diverge with respect to the expected behaviour of solids under strong compression. To illustrate this divergence, one could take the logarithm $\ln(p/p_{FG})$ of the ratio between the pressure predicted by the given EOS form and the pressure of the corresponding Fermi gas $p_{FG} = p_{FGo} \cdot x^{-5}$ for the ultimate asymptotic behaviour. Because this ratio becomes zero at ambient pressure, the logarithm would diverge like ln(1-x) at $x \to 1$, in which $x = (V/V_0)^{1/3}$. A finite value for a modified logarithmic ratio is obtained, if the diverging contribution ln(1-x) is subtracted from $\ln(p/p_{FG})$ to obtain the linearised logarithmic pressure ratio:

$$\eta = \ln(p / p_{FG}) - \ln(1 - x) \qquad (15)$$

This η becomes especially simple for p_{AP2} due to the special constraint given by c_0:

$$\eta_{AP2} = -c_0 \cdot x + \ln\left(1 + c_{AP2} \cdot x(1 - x)\right) \qquad (16)$$

The parameter $c_{AP2} = (3/2)(K_0' - 3) - c_0$ is usually so small that the deviation of η_{AP2} from a linear variation over the whole range $0 \le x \le 1$ is not very strong.

In fact many solids show a very "simple" behaviour [7,8,10,28,32] with $c_{AP2} = 0$ within the experimental accuracy. This means that the first order form AP1 gives in these cases a perfect representation of the experimental (and theoretical) data as shown by the straight line in the corresponding $\eta - x -$ plot for Al in fig. 1 for example. This fig. 1 illustrates the following points:

I. AP1 fits within the given uncertainties the data for Al perfectly over the entire range.

II. Uncertainties estimated from $\Delta K_0'$ remain finite as shown by the "AP2 limits".

III. The form BE2 with the same values for K_0 and K_0' as AP1 diverges rapidly to larger values, but ER2 using the same parameter values diverges in opposite direction.

IV. The form MU2 diverges even more strongly than BE2 and ER2.

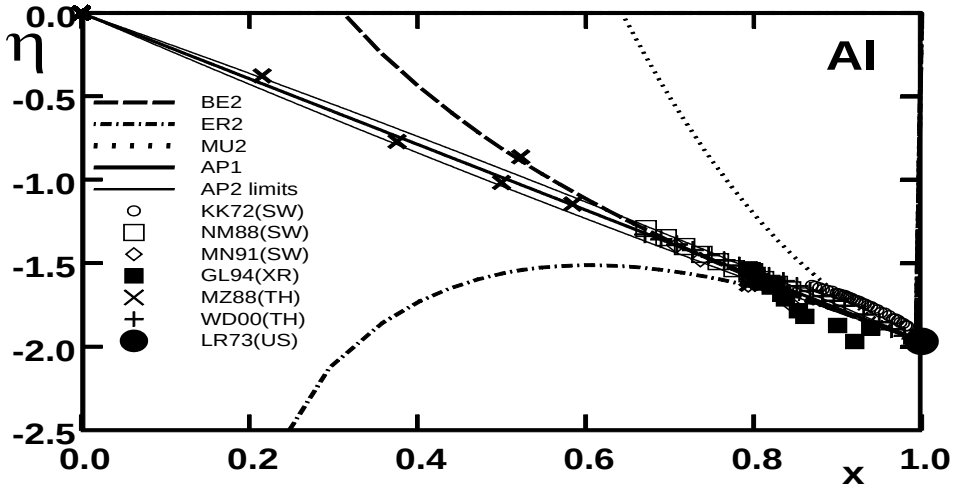

Fig. 1: ü-x-plot for Al with experimental shock wave (SW), X-ray (XR), and ultrasonic (US) data and theoretical value (TH) from the literature given in ref. [10].

Another situation is illustrated in fig. 2 for Na. Due to the fact that $K_0' < 4$ in this case, BE2 diverges to negative values at finite compressions; ER2 shows the wrong curvature and diverges also rapidly. MU2 has the correct curvature, but diverges even more rapidly.

A third situation with different curvature, typical for rare gas solids and molecular solids [8], is illustrated in fig. 3 for hydrogen with theoretical (TH), neutron diffraction (ND), X-ray diffraction (XD), volumetric (VO) and ultrasonic data (US). Detailed references are given in the original work [8]. ER2 is here appropriate for a wide range in compression as expected from the simple exponential repulsion typical for closed shell configurations with very weak (Van der Waals) attraction. BEL needs definitely higher order terms going beyond BE2. MU2 is reasonable only in a very limited range of compression, but AP2 fits perfectly to all the experimental and theoretical data given here for H_2 at 0 K.

In conclusion, AP2 appears to be flexible enough to represent experimental and theoretical EOS data for "regular" solids over extremely wide ranges in compression. A

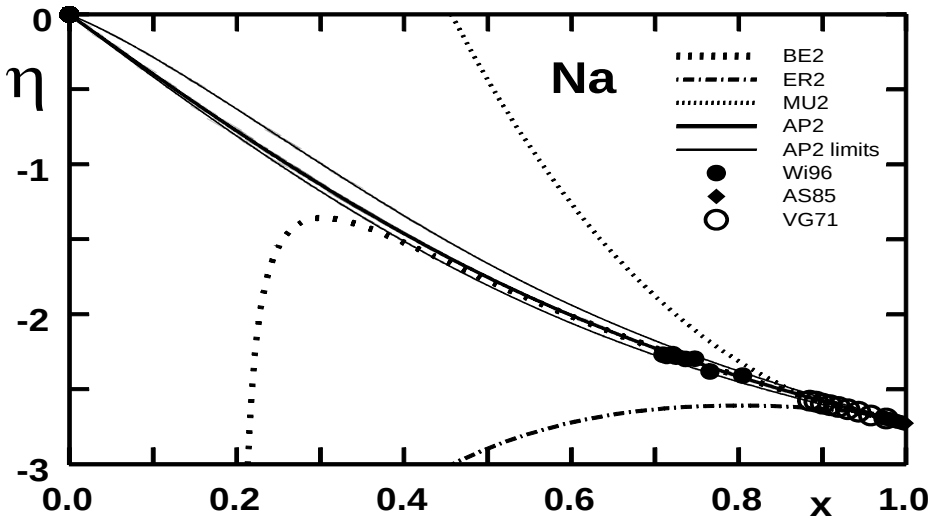

Fig. 2: ü-x-plot for Na with experimental data from the literature given in ref. [10].

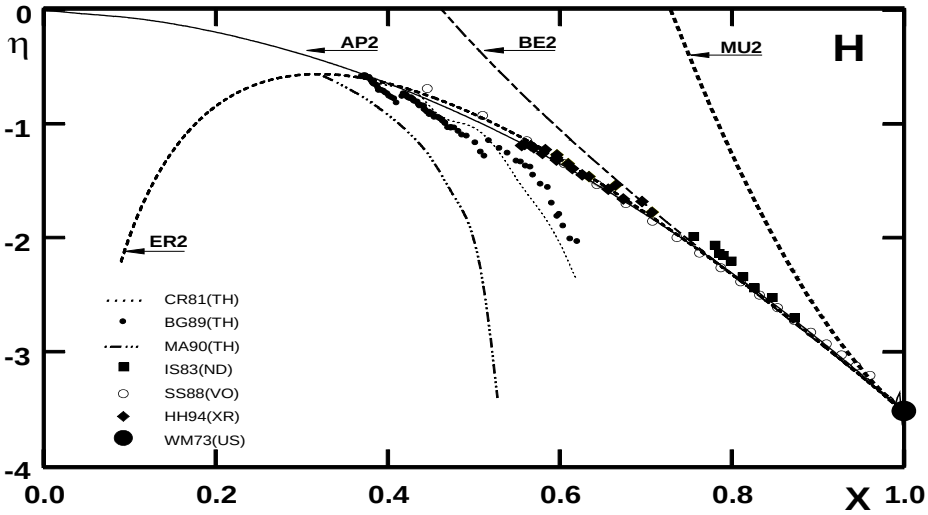

Fig. 3: ü-x-plot for hydrogen with theoretical (TH), neutron diffraction (ND), X-ray diffraction (XD), volumetric (VO) and ultrasonic (US) data from the literature given in ref. [10].

further constraint with respect to experimental values for the cohesive energy requires only one more free parameter provided by the form AP3.

Anomalous EOS relations for solids with continuous electronic transitions such as Ce above its critical point for the α-γ-transition, taken as just one example for a heavy fermion system, require special treatment [10]. Furthermore, very precise representations of different isotherms of one given substance will also require more than just temperature dependent parameters $V_0(T)$, $K_0(T)$ and $K_0'(T)$ in a parametric AP2 form [33], this point is treated in detail at the end of the next section.

3. Mie-Grüneisen EOS and anharmonic corrections

3.0 GENERAL REMARKS

In the parametric EOS forms discussed in the last section, the effects of temperature are treated only by the use of temperature dependent parameters without any theoretical justification for the special form of these temperature dependencies. Therefore extrapolations beyond the range of the fitted data diverge rapidly in these cases.

Statistical thermodynamic methods for solids offer a rigorous basis for the calculation of all the thermo-physical properties from a thermodynamic potential, as discussed in the introduction. Effects of different approximations can be studied systematically. In this scheme one starts from the volume dependent ground state energy of the solid (usually related to the energy of the static ideal lattice $E_{sl}(V)$) and adds successively contributions from different excitations. The first set of excitations is usually provided by the lattice vibrations or in quantised form by the phonon contributions. Electronic excitations are usually neglected in insulators. However, in metals significant contributions come also from the conduction electrons. Magnetic excitations as well as contributions from defects are mostly neglected, and in most cases all the excitations are treated as excitations of independent quasiparticles. This means that phonon-phonon as well as electron-phonon interactions are usually not taken into account.

The various steps from the Hamiltonian of an (idealised) solid via the partition function to the free energy of the solid have been worked out in many textbooks on solid-state physics and thermodynamics as mentioned in the introduction. The essential feature for the present discussion is only the fact that the total free energy F(V,T,N,…) can be split by these procedures into the ground state contribution of the static lattice $E_{sl}(V,N,\ldots)$ and into additional contributions for the various types of excitations:

$$F(V,T,N) = E_{sl}(V,N) + F_{ph}(F,T,N) + F_{el}(V,T,N) + \ldots \qquad (17)$$

$F_{ph}(V,T,N)$ represents here the free energy of the phonons and includes zero point contributions. $F_{el}(V,T,N)$ represents the free energy of the conduction electrons. All other excitations like magnons and lattice defects as well as mutual interactions like phonon-phonon or electron-phonon coupling are neglected for simplicity. The Maxwell relation for the calculation of the pressure $p = -\partial F/\partial V\big|_{T,N}$ preserves the separation into the three different terms:

$$p(V,T) = p_{sl}(V) + p_{ph}(V,T) + p_{el}(V,T) \qquad (18)$$

The same separation holds also for the internal energy U(V,T,N), the entropy S(V,T,N) and the other thermodynamic potentials discussed in the introduction.

The next steps in the description of the thermophysical properties of solids involve:
I. The specification of the static lattice energy (for instance by a model for the interatomic interactions) or the equivalent selection of a specific (parametric) EOS form for the static lattice.
II. A specific model for the excitation spectrum of the phonons.
III. An additional model for the excitation spectrum of the conduction electrons.
Point I was discussed already in the section 2. Points II and III are the subjects of the next subsections.

3.1 THE MIE-GRÜNEISEN APPROCH

The simplest approach for a quantum mechanical treatment of the lattice vibrations and the corresponding temperature dependence of the specific heat was proposed by Einstein [34] in 1907. Einstein assumed that the whole phonon spectrum could be represented by just one characteristic (average) frequency, later called the Einstein frequency ν_E or in terms of a characteristic temperature the Einstein temperature $\theta_E = h \cdot \nu_E / k$ with Planck's h and Boltzmann's k.

Grüneisen [35] realised that Einstein's approach was not perfect. Like Einstein, he introduced only one characteristic temperature $\theta(V)$ and in addition the corresponding Grüneisen parameter

$$\gamma_\theta = -\partial \ln \theta / \partial \ln V \big|_T \tag{19}$$

Furthermore, Grüneisen assumed that $\theta(V)$ depends only on volume and not on temperature at constant volume. With this assumption he obtained for the phonon pressure the relation:

$$p_{ph}(V,T) = \gamma_\theta(V) \cdot 3 \cdot N \cdot k \cdot (\theta(V)/V) \cdot u_{ph}(T/\theta) \tag{20}$$

in which the scaled internal energy function $u_{ph}(t)$ was not fixed to Einstein's form, but taken as a material characteristic function depending only on the dimensionless, scaled temperature variable $t = T/\theta(V)$. With the relations (18) to (20) he obtained for the thermal (volume) expansivity $\alpha(V,T)$ the well-known Grüneisen relation:

$$\gamma_{th}(V,T) = \alpha(V,T) \cdot V \cdot K_T(V,T) / C_V(V,T) \tag{21}$$

where $K_T(V,T)$ is the isothermal bulk modulus, $C_V(V,T)$ is the molar (or atomic) heat capacity at constant volume, and V is the molar (or atomic) volume, respectively. It should be noted that $\gamma_{th}(V,T) \Rightarrow \gamma_\theta(V)$ within the Grüneisen approximation!

In other words, $\gamma_\theta(V_0(T))$ at ambient pressure increases only slightly with temperature due to the thermal expansion given by $V_0(T)$. Within the Grüneisen approximation, $\gamma_{th}(V_0(T),T)$ defined by the eq. 21 shows just the same small increase with temperature. A detailed analysis of the temperature dependent of γ_{th} at ambient pressure serves therefore often as a proof for the validity of the Grüneisen assumption.

If one rewrites eq. 20 in terms of the internal energy for the phonons $U_{ph}(V,T)$ one can define another "thermobaric" Grüneisen parameter:

$$\gamma_{tb}(V,T) = p_{ph}(V,T) \cdot V / U_{ph}(V,T) \tag{22}$$

Again, within the Grüneisen approximation $\gamma_{tb}(V,T) \Rightarrow \gamma_\theta(V)$ and from this point of view eq. 22 is often cited as Mie-Grüneisen EOS. On the other hand, eq. 22 is only a definition of γ_{tb} and can be cited as Mie-Grüneisen EOS only when the additional (essential) assumption holds that $\gamma_{tb}(V,T) = \gamma_{th}(V,T) = \gamma_\theta(V)$ independent of temperature at constant volume!

In fact, a specific form for the phonon **D**ensity **O**f **S**tates (DOS) was not required in the Mie-Grüneisen approach. Only Debye [36] introduced a characteristic phonon DOS with a sharp frequency cut-off at the Debye frequency ν_D or temperature θ_D and only the single Debye-Grüneisen parameter $\gamma_D = -d \ln \theta_D / d \ln V$ determines all the volume

dependences of the different phonon frequencies ν_i also in this case. In other words, also Debye assumed that all the (later called) "mode Grüneisen parameters"

$$\gamma_i = -\partial \ln \nu_i / \partial \ln V \big|_T \tag{23}$$

are represented by a single Debye-Grüneisen parameter γ_D. The Debye model leads therefore also to a Mie-Grüneisen EOS with $\gamma_{th} = \gamma_{tb} = \gamma_\theta = \gamma_D$, however with a specially restricted form for the phonon DOS.

3.2 DEFICIENCIES OF THE DEBYE APPROXIMATION

Obviously the Debye approximation [36] represents a major improvement with respect to the Einstein approximation, but its phonon DOS is only a rough approximation for the situation in any real solid. As an example, fig. 4 [6] illustrates that the phonon DOS from a lattice dynamical calculation (LD) for MgO shows much more structure than corresponding the Debye phonon DOS. Typically, the centre of gravity (the "average" frequency) of this phonon DOS would be represented by the Einstein frequency ν_E. In terms of the density of states, the Einstein model is represented in fig. 4 by a delta-function located at ν_E.

The deficiencies of the Debye model are represented in the literature [6] by temperature dependent Debye temperatures indicating that the specific heat at low temperature gives a different Debye temperature in the Debye function than the specific heat at high temperature. In other words, a fit of the low frequency section

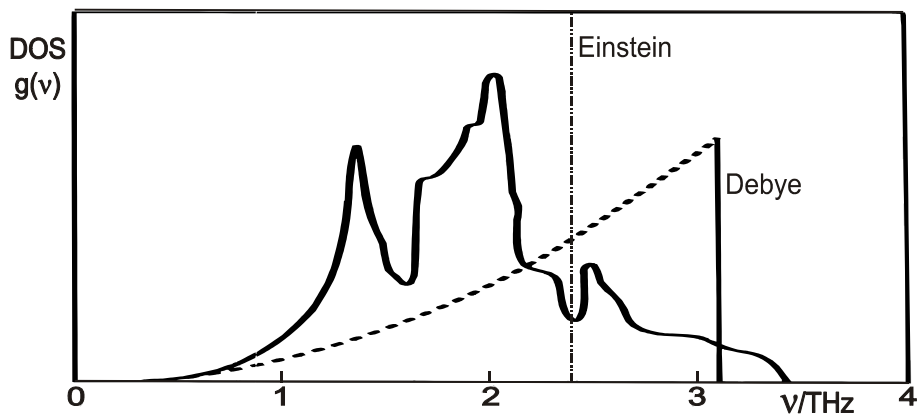

Fig. 4: Phonon DOS for MgO from the Debye approximation compared with lattice dynamical calculations (LD) from the literature [6] and with the corresponding Einstein frequency $\tilde{a}_E$.

of the phonon DOS by the Debye approximation results in an acoustic (or low temperature) Debye temperature θ_{Dacc}, which can deviate significantly from the high temperature value of the Debye-temperature $\theta_{D\infty}$. This $\theta_{D\infty}$ is usually related to the Einstein-temperature θ_E by a factor 4/3 giving $\theta_{D\infty} = 4/3 \cdot \theta_E \neq \theta_{Dacc}$. This problem of a temperature dependent characteristic temperature is just an artefact of the Debye model and can be avoided easily [37] by the use of a slightly more realistic phonon DOS than provided by the Debye model.

3.3 THE OPTIMISED-PSEUDO-DEBYE-EINSTEIN MODEL: opDE

From the discussion in the last section, it should be clear that a slightly more realistic representation of the phonon DOS in comparison with the phonon DOS of the Debye model needs at least two characteristic frequencies or two related temperature parameters. In fact, it is common practice [37] to represent some part of the low frequency phonon DOS by a Debye approximation with the addition of one or several Einstein frequencies for the high frequency part. However, it is computationally more elegant to replace the Debye contribution by a "pseudo-Debye" contribution [33], which corresponds to a bell shaped form of the phonon DOS and to a much simpler function for the phonon internal energy with the correct T and T^4 behaviour at high and low temperatures, respectively. In a first attempt along this direction [33], a Simple-Pseudo-Debye form (SPD) was tested for the normalised internal energy of the phonons $u_{SPD} = U_{ph}/(3Nk \cdot \theta)$ with the normalised temperature $t = T/\theta$ and neglecting zero point contributions for the moment:

$$u_{SPD}(t) = t^4/(a+t)^3 \qquad (24)$$

where $a = (5/\pi^4)^{1/3} = 0.3716$ with $\theta = \theta_{Dacc}$ results in a perfect fit of the Debye C_V at very low temperatures, but a = 0.17 represents a better compromise for a wider temperature range as shown in fig. 5. A better fit of the Debye C_V is obtained, however, if one uses more free parameters. The Pradé-Approximation

$$u_{PA}(t) = t^4/(a_0 + a_1 t + a_2 t^2 + t^3) \qquad (25)$$

for instance with $a_0 = a^3$, $a_1 = 3a^2$ and $a_2 = 3a$ reproduces U_{SPD}, but $a_0 = .068$, $a_1 = a_2 = 0$ result in a Modified-Pseudo-Debye form, U_{MPD}, which shows a more favourable behaviour at low temperatures and at first an unreasonable hump at higher temperature as illustrated in fig. 5 by the curve C_{MPD}. As we will see later, this hump provides however an excellent fit of the Debye form C_{VD}, when the pseudo-Debye form C_{MPD} is combined with an Einstein term as optimised-pseudo-Debye-Einstein form (opDE). A direct fit of C_{PA} related to the Pradé-form u_{PA} results in a = 0.30, $a_1 = 0.07$ and $a_2 = 0.38$ and in a very good representation of the Debye C_{VD}, as shown in fig. 5, where the curve C_{PA} just overlaps perfectly with Debye form.

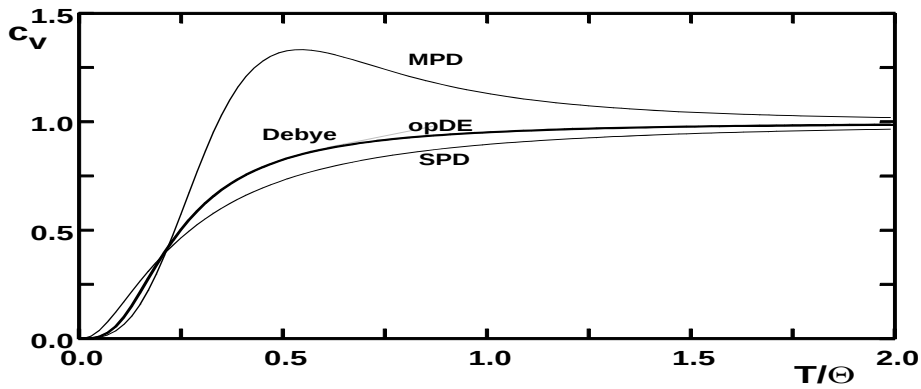

Fig. 5: Normalised specific heat data for the Debye model, $c_{VD} = C_{VD}/(3Nk)$ and for the three different pseudo Debye forms, c_{SPD}, c_{MPD}, and c_{opDE}, related to the forms u_{SPD}, u_{MPD}, and u_{opDE} as explained in the text.

In comparison with the Debye approximation, the additional free parameters a_0, a_1 and a_2 in u_{PA} would allow us to fit also a more realistic phonon DOS than provided by the Debye model. However, for practical reasons, it is more convenient to combine an u_{MPD} contribution for low temperatures (low frequencies) with just one Einstein term for high temperatures (high frequencies):

$$u_{opDE}(t,f) = g \cdot t^4 / (a_0 \cdot g + t^3) + (1-g) \cdot f / (e^{f/t} - 1) \qquad (26)$$

In the fit of the corresponding C_{opDE} to the Debye C_{VD} the frequency ratio $f = \nu_E / \nu_D = \theta_E / \theta_D$ is constrained by the selection of the weight g for the Modified-Pseudo-Debye term to

$$f = (3/4)(1-g^{4/3})/(1-g) \qquad (27)$$

With this constraint, the best fit for C_{opDE} is obtained for g = 0.068 with a_0 = .0434 and the deviation from C_{VD} is so small that it can not be seen in fig. 5, but only in fig. 6, which shows an enlarged difference plot (opDE). For comparison, this plot includes also the result for a similar fit of a SPD term with an Einstein term (spDE) and the difference (PA) between C_{PA} and C_{VD}.

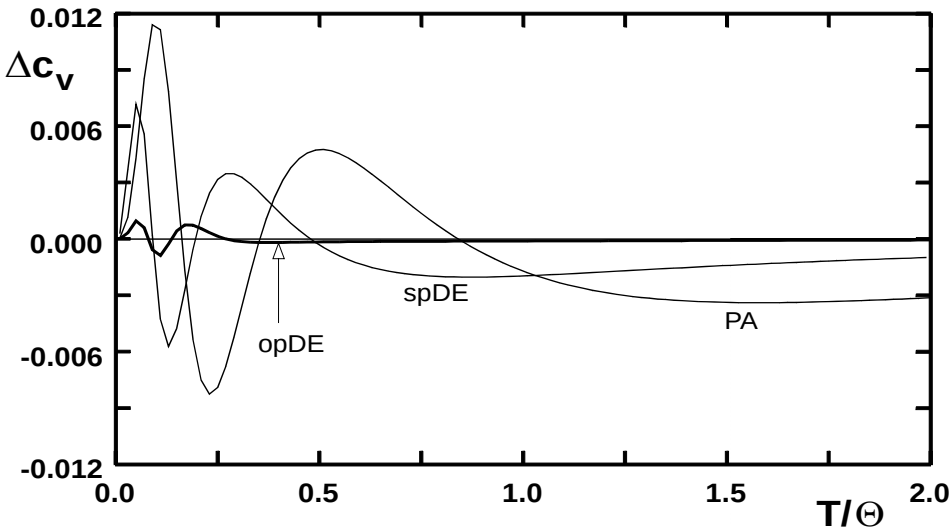

Fig. 6: Differences of specific heat curves with respect to c_{VD} based on three different pseudo-Debye models i) based on the forms u_{opDE}, ii) based on a similar SPD-Einstein model, and iii) based on the form u_{PA}.

Two points should be noted:

I. The opDE approximation (eq. 26) represents the normalised Debye c_v with absolute deviations smaller than 0.003 or smaller than $3^o/_{oo}$ for $T > 0.13 \cdot \theta_D$ This accuracy seems to be much better than the experimental accuracy for c_v-values and the deviations for $T < 0.1 \cdot \theta_D$ have no effect on the representation of EOS data, because the thermal pressure of the phonons is almost zero in this range.

II. Both the adapted SPD-Einstein form and the Pradé approximation show larger deviations from the Debye form as shown in fig. 5.

III. For a real solid with deviations from the Debye phonon DOS, it is therefore most convenient to use the opDE approximation (eq. 26) with fixed the weight g = 0.068 and

a fit of the Einstein frequency ratio f (or a few f_i) to the actual data. In this case θ corresponds still to θ_{Dacc} and the fitted value of f gives for high temperature limit:

$$\theta_{D\infty} = \theta_{Dacc} \cdot (g^{4/3} + (1-g) \cdot f \cdot 4/3) \tag{28}$$

This means that a Mie-Grüneisen model can be applied to solids with phonon DOS deviating significantly from the Debye case; no (artificial) temperature dependence occurs in the characteristic (Mie-Grüneisen) temperature θ.

3.4 DEFICIENCIES OF THE MIE-GRÜNEISEN MODEL

With the opDE model, one can avoid the deficiencies of the Debye model in a manner, which is very convenient in practical applications to be discussed in section 4. However, the Mie-Grüneisen model has also some minor deficiencies, which are not yet taken into account in the opDE approach:

I. The Mie-Grüneisen approach considers only the volume dependence of one characteristic (average) frequency $\nu_\theta = k \cdot \theta / h$ by the corresponding γ_θ. Differences in the mode Grüneisen parameters can be taken into account in the opDE model by different mode Grüneisen parameters for θ_{Dacc} and θ_∞ (eq. 28) or, in other words, by the use of one (or several) volume dependent f (or f_i). In cases like Si and Ge with negative acoustic mode Grüneisen parameters, this could be an interesting application for a modified opDE model; however, in most cases these effects are much to small to show up in the thermal pressure (within the given experimental accuracy).

II. For minerals [37] or other solids with complicated phonon-DOS an extended opDE model with several f_i and corresponding γ_i could be of interest to include differences in the mode-Grüneisen parameters for the acoustic and the different optical branches; however, in the present approach these modifications are considered to present only minor changes.

III. Explicit temperature dependencies in the phonon frequencies (at constant volume) $a_i = \partial \ln \nu_i / \partial T|_V \neq 0$ represent "intrinsic" anharmonic contributions [38], which are not taken into account by the usual Mie-Grüneisen model. These contributions can lead to new effects, which can be treated in the following way:

This explicit anharmonicity (in addition to the anharmonicity treated already in the quasiharmonic approximation by finite values for the mode Grüneisen parameters) shows up first of all in deviations of the specific heat C_v at high temperatures from the classical Dulong-Petit value (3Nk for monatomic solids). Recently [30,39,40] it was shown that an average explicit anharmonic contribution can be included to first order as a deviation from the Mie-Grüneisen model by replacing θ(V) by a temperature dependent "anharmonic"

$$\theta_a(V,T) = \theta(V) \cdot (1 - A \cdot u(T/\theta(V))) \tag{29}$$

where u represents the quasiharmonic thermal contribution of the phonons to the internal energy in normalised form:

$$u(t) = U_{qh}(T,V)/(3Nk \cdot \theta(V)) \tag{30}$$

with t = T/θ(V). The volume dependence $\gamma_A = -d\ln A / d\ln V \neq 0$ of the anharmonicity parameter A is often neglected. However, if one works out the effects of A and γ_A on all the thermodynamic relations [40] one finds that

$$\gamma_{tb}(t) = \gamma_\theta - A \cdot \gamma_A \cdot u(t) \qquad \text{and} \qquad \gamma_{th}(t) = \gamma_\theta - 2 \cdot A \cdot \gamma_A \cdot u(t) \qquad (30)$$

One may notice that γ_θ keeps its pure volume dependence (by definition), but both γ_{tb} and γ_{th} are modified by some extra explicit temperature dependence. In other words, the Mie-Grüneisen relation $\gamma_\theta = \gamma_{tb} = \gamma_{th}$ is violated by $\gamma_A \neq 0$. This means that an explicit anharmonic contribution with constant A does not yet violate the Mie-Grüneisen relation; however, $\gamma_A \neq 0$ goes beyond the Mie-Grüneisen approach.

The effects of this explicit anharmonicity are finally worked out in the evaluation of experimental data with the software discussed in section 4. In metals, effects of this explicit anharmonicity are masked to some extend by thermal contributions from conduction electrons. Therefore, these effects have to be considered also in any detailed analysis of EOS data for metals.

3.5 THERMAL CONTRIBUTIONS FROM CONDUCTION ELECTRONS

The contribution of conduction electrons to the heat capacity in "normal" metals is given in many textbooks in the form of a free electron approximation by

$$C_{ce} = Nk \cdot (\pi^2 / 2) \cdot (T / T_F^*) \qquad (32)$$

where N represents the number of atoms and $T_F^* = T_F / n_{ce}$ is an effective Fermi temperature, which is related to the actual Fermi temperature T_F by scaling with the number of conduction electrons per atom n_{ce}. In "normal" metals, T_F^* is very large with respect to the melting temperature which means that C_{ce} gives a small contribution to the total heat capacity at high temperatures in these cases; only at very low temperatures does C_{ce} dominate over the phonon contribution, which decreases as T^3. In "heavy fermion systems" T_F^* may become smaller than the melting temperature and eq. 32 needs then some modifications at elevated temperatures. In other words, these cases may need special attention and are excluded here. The contribution of the conduction electrons to the thermal pressure depends on the value of $\gamma_{ce} = -d \ln T_F^* / d \ln V$, which is known only for a few metals [41]. For a Fermi gas of free electrons $\gamma_{FG} = 2/3$; however, for real metals positive and negative values of about this magnitude can be expected [41]. With these values of γ_{ce} for "normal" metals, one can neglect the possible contribution of the conduction electrons to the thermal pressure; however, in the evaluation of shock wave data, the conduction electrons act like a heat sink and their effect on the temperature along the shock Hugoniot cannot be neglected [41].

4. Software for the calculation and fitting of EOS data

4.0 THE SCHEME

The present program is based on the intention to calculate not only the EOS data but also all the thermophysical properties by a state-of-the-art representation of the free energy F(V,T,N) (as thermodynamic potential of the system) with a minimum number of free parameters. This approach needs the following parameters:

I. For the energy (and pressure) of the static lattice

I.1 The cohesive energy contribution : E_{0sl}

I.2 The equilibrium volume per atom : V_{0sl}

I.3 The corresponding bulk modulus : K_{0sl}

I.4 its pressure derivative : K'_{0sl}

I.5 the atomic number for APL : Z
(APL for compounds needs Z as total number of electrons in the cell volume V_{0sl})

II. For the phonon contributions

II.1 The acoustic Debye temperature : $\theta_{Dacc} = \theta$

II.2 The Grüneisen parameter of θ_{Dacc} : γ_θ

II.3 For $\theta_{D\infty} / \theta_{Dacc}$ a frequency ratio : f

II.4 The explicit anharmonicity parameter : A

II.5 The Grüneisen parameter of A : γ_A

III. For the conduction electrons:

III.1 The effective Fermi temperature : T_F^*
(for $C_{ce}/T = \Gamma_{ce} = (\pi^2/2) \cdot R / T_F^*$)

III.2 The Grüneisen parameter of T_F^* : γ_{ce}

IV. The atomic mass number : M
(or the mass number per unit cell)

V. For the boundary of the solid-state region:

V.1 The melting temperature at zero pressure : T_{m0}

V.2 The Grüneisen parameter of T_m : γ_{m0}

For an insulator this implies 9 essential parameters (I.1-I.4 and II.1-II.5) in the representation of all the thermo-physical properties including the p(V,T) - EOS over the entire region of stability for the solid. For the EOS alone only 8 parameters are needed. The cohesive energy is included here only for later discussions of phase transitions from the presently described low-pressure phase to possible high-pressure phases. For these considerations space is kept for an additional parameter D_0 describing the energy difference between the minima of the static lattice energies of the two phases.

4.1 DETAILS OF THE PROGRAM

The present program package includes one program **TEOScalc** for the calculation of thermo-physical properties from the input file **TPpropE** that contains all the parameters listed above. A second program **TEOSfit** is use to determine most of these parameters from input data for $V_0(T)$, $\alpha_0(T)$, $K_0(T)$ and $C_{p0}(T)$. Both programs are written in Mathcad 2000i and can be downloaded from the website www.EOSdata.de. This website provides also the data file **TPpropE**, which lists the 18 parameters at present just for a few elements, but we are working on the completion of this list and anyone using this program is encouraged to send us new data, which we would implement with reference to the authors on a second sheet.

If one uses the program for the first time, one finds that it is set up at present for Argon. For other the 18 for Argon in **ZA:=18** must be replaced by the atomic number for the desired element to read the corresponding data from **TPpropE**. Later in the program various steps are marked, where one can select temperature and pressures for the calculation of any isotherm or isobar. When the cohesive energy E_0 is given for the element, the program determines at first all the parameters for an AP3-type isotherm by the use of the input parameters Z, Vr, Kr, Kr' for the reference state (pr, Tr) (usually 0 GPa and 0 K) and E_0 is used to calculate the third parameter c_3 with a simple approximation for the function $E1(x) = \int_x^\infty e^{-t}/t \cdot dt$ provided by Segeletes [42]. The volume dependence of θ and γ_θ is calculated by the use of the Barton-Stacey form [43], which we consider most appropriate for many reasons. With γ_θ, θ, and f the phonon pressure due to zero point motion is calculated and use in the determination of the parameters V_{0sl}, K_{0sl}, and K'_{0sl} for the static lattice. $V_0(T)$ is determined from the reference EOS with the corresponding phonon pressure calculated in the opDE approximation. With $V_0(T)$ and the phonon pressure from the opDE approximation K(T,V) and $K_0(T)$ are also calculated. It should be noted that the common approximation $K_0(T) = K_r \cdot (V_r / V_0(T))^{K'_r}$ represents only the dominant change and differs from the exact calculation!

As an example for the results provide by the program **TEOScalc**, fig. 7 show some selected isobars for Ar and fig. 8 illustrates the variation of the different Grüneisen parameters with temperature at two different pressures.

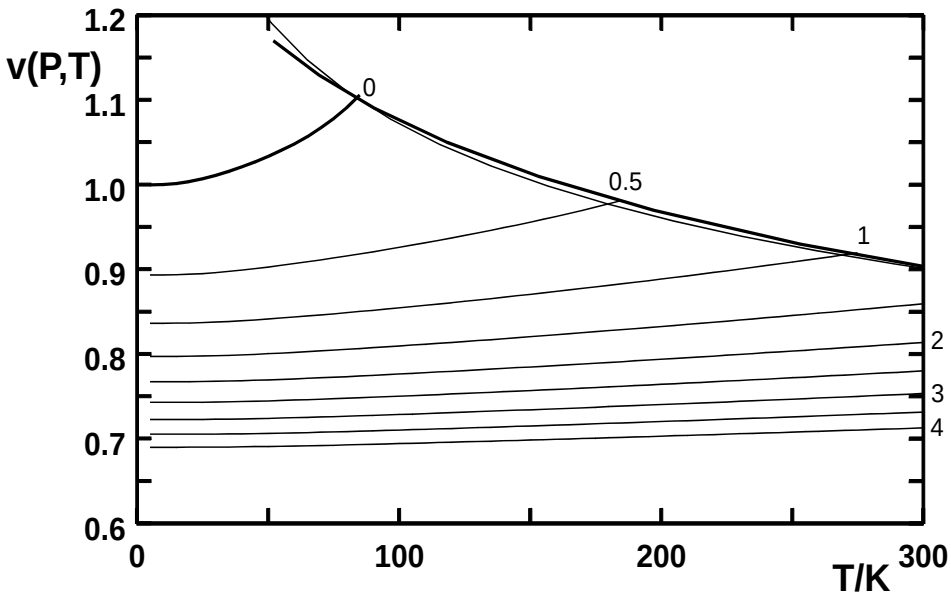

Fig. 7: Calculated isobars v(p,T) = V(p,T)/Vr of Ar for p = 0 to 4 GPa in steps of åp = 0.5 GPa. Two slightly different rough estimates of the melting curve are included to limit the range of reasonable data.

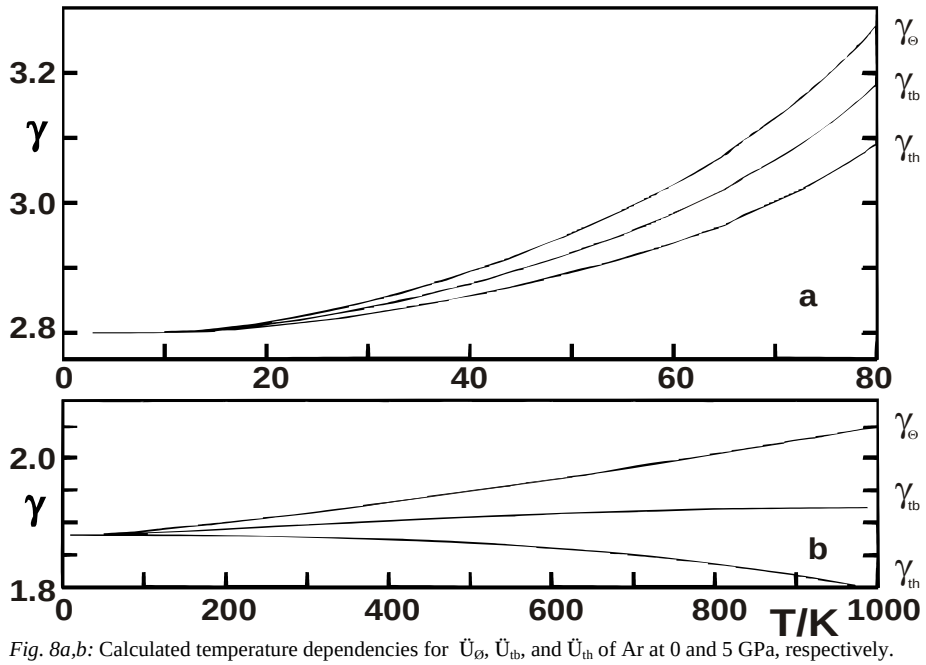

Fig. 8a,b: Calculated temperature dependencies for $\ddot{U}_{\varnothing}$, $\ddot{U}_{tb}$, and $\ddot{U}_{th}$ of Ar at 0 and 5 GPa, respectively.

The program **TEOSfit**, on the other hand, determines some of the parameters stored in the **TPpropE** by a correlated fit of thermophysical data for a given element (or compound). At first the available incomplete or not yet refined data from **TPpropE** and the experimental data for $C_{p0}(T)$, $V_0(T)$ and $K_0(T)$ are read by the program. At this point, one has to check whether the data files for C_{p0}, V_0, and K_0 cover the same temperature ranges with the same steps in temperature. Since this is usually not the case, one has to fit first these data individually (without a deeper physical meaning of these fits) to get "experimental" data of C_{p0}, V_0, and K_0 for equal temperatures. This section is labelled "preliminary" parametric representation of $V_0(T)$, $\alpha_0(T)$, and $K_0(T)$. These fit starts with a determination of θ_0 from C_{p0} - data with the opDE-form for C_v and a parametric $C_{p0} - C_{V0}$ correction. With the best parametric fits for V_0, α_0, K_0 and C_{p0} "experimental" values for γ_{th} and for the $\alpha \cdot \gamma_{th} \cdot T -$ correction are calculated and used for the determination of the frequency parameter f and for the anharmonicity parameter A from the fit of the $C_{p0}(T)$ data. Finally, $\gamma_{\theta 0}$ and the second anharmonicity parameter γ_A are determined from a correlated fit of the data for $V_0(T)$, $\alpha_0(T)$ and $K_0(T)$. Since, the initial fit of the $C_{p0}(T)$ used the "experimental" values for γ_{th}, a second circle (refinement) is added with the best-adjusted values for $\gamma_{\theta 0}$ and γ_A. The program provides finally figures for the comparison of experimental and calculated values for $C_{p0}(T)$, $V_0(T)$, $\alpha_0(T)$, and $K_0(T)$ and ends with a compilation of the best-fitted parameters to be transferred into the data file for the elements.

4.2 APPLICATIONS

So far we have applied the **TEOSfit**-program in the present and some preliminary version to rare gas solids [30], to data for Cu, Ag, and Au [39], and to some common pressure calibrants like NaCl, MgO, CsCl and Al_2O_3 [43]. Due to the modifications of the program in the process of its development minor numerical changes may occur in a re-evaluation of these data, but we hope, that future uses of this program package will help to establish a reliable database for the calculation of all the thermo-physical properties for the elements at any pressure or temperature.

5. Conclusion

On the basis of a rigorous physical model the present EOS formulation allows for safer extrapolations to higher pressures and temperatures. A meaningful representation of the quasiharmonic phonon contribution with the optimised pseudo Debye-Einstein model in the frame work of the Mie-Grüneisen approximation allows for additional explicit anharmonic corrections, which are essential for accurate extrapolations into the high temperature region. Since the volume dependence of this anharmonicity A(V) given by the parameter γ_{A0} is still somewhat uncertain, a comparison with theoretical studies of this parameter for extended regions in pressure and temperature is very desirable. First attempts along this line show indeed that Molecular Dynamics [45] and modern Statistical Dynamics [46] calculations can help to understand the volume dependence of the explicit anharmonic contributions, but in any case, the semi-empirical representation of these anharmonic contributions in the present approach remains most useful for the handling of EOS data [47].

6. References

1. Falk, G. (1990) *Physik - Zahl und Realität*, Birkhäuser, Basel.
2. Zharkov, V.N., and Kalinin, V.A. (1971) *Equations of State for Solids at High Pressure and Temperatures*, Consultants Bureau, New York.
3. Stacey, F.D., Brennan, B.J., and Irvine, R.D. (1981) Finite strain theories and comparisons with seismological data, *Geophysical Surveys* **4**, 189-232.
4. Godwal, B.K., Sikka, S.K., and Chidambaram, R. (1983) Equations of state theories of condensed matter up to about 10 TPa, *Phys. Rep*. **102**, 121- 197.
5. Eliezer, S., and Ricci, R.A. (1991) *High-Pressure Equations of State: Theory and Applications*, Elsevier Science Publishers, Amsterdam.
6. Anderson, O.L. (1995) *Equations of State for Geophysics and Ceramic Science*. Oxford University Press, New York.
7. Holzapfel, W.B. (1996) Physics of solids under strong compression, *Rep. Prog. Phys.* **49**, 29-90.
8. Holzapfel, W.B. (1998) Equations of state for solids under strong compression, *High Press. Res.* **16**, 81-126.
9. Poirier, J.-P. (1990) *Introduction to the Physics of the Earth's Interior*, Cambridge University Press, Cambridge.
10. Holzapfel, W.B. (2001) Equations of state for solids under strong compression, *Z. Kristallogr*. **216**, 473-488.
11. Murnaghan, F.D. (1937) Finite deformations of an elastic solid, *Am. J. Math*. **59**, 235-260.
12. Murnaghan, F.D. (1944) The compressibility of media under extreme pressure, *Proc. Natl. Acad. Sci. USA* **30**, 244-247.
13. Freund, J., and Ingalls, R. (1989) Inverted isothermal equations of state and determination of Bo, B'o and B"o, *J. Phys. Chem. Solids* **50**, 263-268.

14. Baonza, V.G., Cäceres, M., and Nunez, J. (1995) Universal compressibility behaviour of dense phases, *Phys. Rev. B* **51**, 28-37.
15. Birch F. (1947) Finite elastic strain of cubic crystals, *Phys. Rev*. **71**, 809-824.
16. Vinet, P., Ferrante, J., Smith, J.R., and Rose, J.H. (1986) A universal equation of state for solids, *J. Phys. Condens. Matter* **19**, L467-L473.
17. Slater, J.C., and Krutter, H.M. (1935) The Thomas-Fermi method for metals, *Phys. Rev*. **47**, 559-568.
18. Feynman, R.P., Metropolis, N., and Teller, E. (1949) Equation of state of elements based on the generalized Fermi-Thomas Theory, *Phys. Rev*. **75**, 1561.
19. Salpeter, E.E, and Zapolsky, H.S. (1967) Theoretical high-pressure equations of state including correlation energy, *Phys. Rev*. **158**, 876-886.
20. Landau, L.D., and Lifshitz, E.M. (1980) *Statistical Physics. Part 1-3rd ed.*, Pergamon Press, Oxford.
21. Stacey, F.D. (2000) The J-primed approach to high-pressure equations of state, *Geophys. J. Int.* **143**, 621-628.
22. Mie, G. (1903) Zur kinetischen Theorie der einatomigen Körper, *Ann d. Phys*. **11**, 657-697.
23. Jones, J.E. (1924) On the determination of molecular fields, *Proc. Roy. Soc. (London)* **A106**, 441-462.
24. Born, M., and Mayer, J. (1932) Zur Gittertheorie der Ionenkristalle, *Z. Physik* **75**, 1-18.
25. Morse, Ph.M. (1929) Diatomic molecules according to the wave mechanics. II. vibrational levels, *Phys. Rev*. **34**, 57-64.
26. Rydberg, R. (1932) Graphische Darstellung einiger bandenspektroskopischer Ergebnisse, *Z. Physik* **73**, 376-385.
27. Vinet, P., Rose, J.H., Ferrante, J., and Smith, J.R. (1989) Universal features of the equation of state of solids, *J. Phys. Condens. Matter* **1**, 1941-1963.
28. Holzapfel, W.B. (1991) Equations of state for strong compression, *High Press. Res*. **7**, 290-293.
29. Holzapfel, W.B. (2002) Equations of state for regular solids, *High Press. Res*. **22**, 209-216.
30. Holzapfel, W.B., Hartwig, M., and Reiss, G. (2001) Equations of state for rare gas solids under strong compression, *J. Low Temp. Phys.* **122**, 401-412.
31. Holzapfel, W.B. (2003) Comment on „Energy and pressure versus volume: Equation of state motivated by the stabilized jellium model", *Phys. Rev.* **B67**, 026102/1-3.
32. Köhler, U., Johannsen, P.G., and Holzapfel, W.B. (1997) Equation of state data for CsCl-type alkali halides, *J. Phys.: Condens. Matter* **9**, 5581-5592.
33. Holzapfel, W.B. (1994) Approximate equations of state for solids from limited data sets, *J. Phys. Chem. Solids* **55**, 711-719.
34. Einstein, A. (1907) Die Plancksche Theorie der Strahlung und die Theorie der spezifischen Wärme, *Ann d. Phys*. **22**, 180-194.
35. Grüneisen, E. (1912) Theorie des festen Zustandes einatomiger Elemente, *Ann. d. Phys. IV*, 257-306.
36. Debye, P. (1912) Zur Theorie der spezifischen Wärme, *Ann. d. Phys.* **39**, 789-839.
37. Kieffer, S.W. (1979) Thermodynamics and lattice vibrations of minerals. 3. Lattice dynamics and an approximation for minerals with application to simple substances and framework silicates, *Rev. Geophys. Space Phys.* **17**, 35-59.
38. Gillet, Ph., Guyot, F., and Malezieux, J-M. (1998) High-pressure, high-temperature Raman spectroscopy of Ca_2GeO_4 (olivine form): some insight on anharmonicity, *Phys. Earth Planet. Inter*. **58,** 141-154.
39. Holzapfel, W.B., Hartwig, M., and Sievers, W. (2001) Equations of state for Cu, Ag, and Au for wide ranges in temperature and pressure up to 500 GPa and Above, *J. Phys. Chem. Ref. Data* **30**, 515-529.
40. Holzapfel, W.B. (2002) Anharmonicity in the EOS of Cu, Ag, and Au, *J. Phys.: Condens. Matter* **14**, 10525-10531.
41. Table 5.1 and discussion on p. 140 in ref. 2.
42. Segeletes, S.B. (1998) *Army Research Laboratory, Aberdeen, USA*, report number: ARL-TR-1758.
43. Barton, M.A., and Stacey, F.D. (1985) The Grüneisen parameter at high pressure: A molecular dynamic study, *Phys. Earth Planet. Inter*. **39**, 167-177.
44. Ponkratz, U., and Holzapfel, W.B. (2003) (to be presented) *at the AIRAPT conference, Bordeaux*.
45. Oganov, A.R., Brodholt, J.P., and Price, G.D. (2000) Comparative study of quasiharmonic lattice dynamics, molecular dynamics and Debye model applied to $MgSiO_3$ perovskite, *Phys. Earth Planet. Inter*. **122**, 277-288.
46. Karasevskyy, A.I., and Holzapfel, W.B. (2003) Equations of states and thermodynamic properties of rare gas solids under pressure calculated with a self-consistent statistical method, *Phys. Rev. B.* (to be published).
47. *The webpage* **www.EOSdata.de** *is presently in preparation to provide these codes and any question concerning their application should be directed to* **holzapfel@physik.upb.de** **.**